Plant and Soil **201:** 307–320, 1998.

Modelling the influence of assimilate availability on root growth and architecture

Philippe Thaler[1] and Loïc Pagès[2]
[1]*CIRAD-CP, Programme Hévéa, BP 5035, 34032 Montpellier Cedex 1, France and* [2]*INRA, Centre d'Avignon, Unité de Recherche en Ecophysiologie et Horticulture, Domaine St Paul, Agroparc, 84914 Avignon Cedex 9, France**

Received 16 January 1998. Accepted in revised form 20 March 1998

Key words: apical diameter, carbon allocation, *Hevea brasiliensis*, root system architecture, root growth, rubber tree, simulation model, sink strength

Abstract

A model has been designed to simulate rubber seedling root development as related to assimilate availability. Each root of the system is defined both as an element of a network of axes, characterized by its order, position and connections and as an individual sink competing for assimilates. At each time step, the growth of each root is calculated as a function of its own growth potential and of assimilate availability calculated within the whole plant. The potential elongation rate of a root is estimated by its apical diameter, which reflects the size of the meristem. When a root is initiated, the apical diameter depends on root type, but it varies thereafter according to assimilate availability. Thus, the latter controls both current and potential elongation. The model was able to simulate periodicity in root development as related to shoot growth and to reproduce differences in sensitivity to assimilate availability related to root type. It thereby validated the hypothesis that root growth but also root system architecture depend on assimilate allocation and that apical diameter is a good indicator of root growth potential. Provided that specific calibration is done, this model may be used for other species.

Introduction

Root system architecture (shape and structure) determines the ability of the plant to capture and transport soil resources (Caldwell, 1987; Fitter et al., 1991). This architecture results from processes of growth (axial and radial) and branching. Root growth requires carbohydrates originating from the shoot, as the basis of tissue constituents and as a substrate for respiration. Carbon requirements depend on the structure of root systems, since the different types of roots vary in carbon cost (Nielsen et al., 1994). This infers that root architecture affects exploitation efficiency (Berntson, 1994; Nielsen et al., 1994), but also that variations in carbohydrate translocation from the shoot influence the architecture of the root system (Thaler and Pagés, 1996a) and, in turn, soil resource acquisition and transport. Since branching processes are regulated by auxin synthesized in the growing shoots (Wightman and Thimann, 1980), they are also related to shoot development (Thaler and Pagès, 1996a).

For such complex systems, models are useful for testing hypotheses on interacting mechanisms. From the basic concept of 'functional equilibrium' proposed by Brouwer (1962), many authors have developed models in order to simulate the dynamics of plant growth and development as related to resource allocation. However, in most cases dealing with carbohydrate allocation, the root system have been, when not ignored, described without spatial or structural specifications (Buwalda, 1991; Dick and Dewar, 1992).

On the other hand, architectural models consider the root system as a three-dimensional network of individual axes (Diggle, 1988; Pagès and Aries, 1988). They explicitly calculate the branching and elonga-

---

* FAX No.: (33) 04 90 31 60 28. E-mail: Pages@avignon.inra.fr

tion dynamics of each axis in the system. However, functions simulating elongation and branching patterns have no explicit physiological inputs. They use either deterministic (Diggle, 1988; Pagès and Aries, 1988) or stochastic (Fitter et al., 1991; Jourdan et al., 1995; Pagès et al., 1989, 1992) input functions, dealing directly with the morphological variables (e.g. root length vs. time). This feature makes it difficult to establish functional links between root and shoot development, but it also limits the range of application of these models, since it reduces their ability to respond to environmental changes. Some environmental factors such as soil strength have been introduced in models in order to affect elongation as related to local conditions (Pagès et al., 1989), but without correlations with the rest of the system.

Therefore, attempts to merge allocation and architectural models are likely to improve vastly the ability of these models to analyse root development and root–shoot relationships.

On the basis of experimental data (Aguirrezabal et al., 1994), Aguirrezabal and Tardieu (1996) proposed some elements for modelling sunflower root system growth as related to intercepted photosynthetic photon flux density (PPFD). They assumed that root growth is controlled by source activity and source-sink distance. Their data also indicated that a large proportion of branches quickly stop elongating irrespective of intercepted PPFD, and this suggests that sink demand should also be introduced in such models. Clausnitzer and Hopmans (1994) developed an architectural model which links shoot and root growth and activity: water flow allowed by root uptake as related to local conditions determines assimilate input which, in turn, affects shoot and root growth. This model represents an important step since it enables a description of the growth of the different roots as a function of both global environment and local root conditions. But in this model, root growth is still calculated by a predefined growth function (potential) that is modulated by a coefficient representing the local soil constraint and assimilate availability. This type of model cannot account for the extensive variability of root growth patterns, that is encountered even in homogeneous conditions (e.g. Le Roux and Pagès, 1994; Pagès, 1995; Yorke and Sagar, 1970).

In order to improve the ability of models to analyse root development and root–shoot relationship, the work described herein is an attempt to simulate root architecture development as controlled by assimilate availability. Our approach involves considering each root as an individual sink competing for carbohydrates provided by the shoot, but also as an element of a system of axes, specified by its position (topology and time) within the global architecture. Therefore, in the whole plant model designed, the shoot is described roughly in order to define its source and sink properties, whereas the root system part is more detailed. We focused on the determination of each root's elongation potential, but we also took into account radial growth and branching patterns. The present paper particularly analyses the ability of such a model to simulate variations in root development which were observed as related to periodic shoot development of young rubber seedlings (Thaler and Pagès, 1996a).

Model concepts

Framework

Our model is based on the architectural model developed by Pagès et al. (1989), adapted to the rubber tree root system (Pagès et al., 1995). It simulates the three-dimensional architecture in discrete time steps of one day. At each time step, the root system is extended by the application of several developmental processes: emission of new roots (seminal or adventitious), growth (elongation and radial growth), and branching. The root system is represented as a set of segments, each segment being the root part generated during one time step. For each segment, spatial coordinates of extreme points are stored, together with information on the characteristics and position of the segment within the system (i.e. branching order, diameter, date of formation, and connections with other segments). The root typology, established by Le Roux and Pagès (1994), distinguishes eight root types: taproot, early secondary roots (ESR), acropetal secondary roots (ASR), late secondary roots (LSR), tertiary roots for each secondary root type, and quaternary roots. Emission and branching processes are described according to Pagès et al. (1995). The emission process generates the beginning of seminal (taproot and ESR) and adventitious (LSR) axes. Branching produces the ASR acropetally. It is described by the inter-branch distance, and the time lag between initiation and emergence, which are parameters specific to each root type.

The main difference from this previous model lies in the simulation of growth processes. In the present model, axial growth is no longer simulated by a typical function of time, whose parameters are fixed at the beginning of each root's growth. In order to relate root growth to assimilate availability, each root is assumed to be an individual sink competing for carbohydrates. The carbohydrate requirements for growth are satisfied on the basis of the demand of the growing organs, which include the carbohydrate involved in structural growth and the carbohydrate used by growth respiration (see the calculation of demand below). Daily carbohydrate availability after maintenance respiration is calculated together with carbohydrate demand for leaf, stem, and root growth. Growth occurs at the potential rate for all sinks when sufficient carbohydrate is available. If this is not possible, the fraction of growth that can be supported is calculated according to the allocation rule. Two different allocation rules are available in this model.

Allocation with priorities

Our results showed that root growth was depressed during the periods of shoot growth (Thaler and Pagès, 1996a). Moreover, when photosynthesis was restricted by shading, root growth was also depressed, whereas leaf expansion and stem elongation were not, or only slightly, depressed (Thaler and Pagès, 1996b). Such results were in accordance with data showing that photosynthates are preferentially used for the growth of the shoot under light-limiting conditions (Logendra et al., 1990). Generally speaking, a large part of the apparent priorities in carbohydrate allocation is thought to originate in sink-source pathways (Wardlaw, 1990). It is also known that decreases in specific leaf area are associated with assimilate accumulation in the leaf when supply is high (Gary et al., 1993). On the other hand, our measurements showed that stem radial growth was nearly constant. In line with such results, we adopted the hypothesis that the plant can be represented by a series of sinks, in the following order: Leaf expansion – Stem elongation – Stem radial growth – Root elongation – Growth in leaf specific mass – Root radial growth. The demand of one sink begins to be fulfilled when the demand of the preceding sink is fully satisfied.

Allocation without priorities

With this concurrent rule, allocation is controlled only by sink demand (which can implicitly include the influence of transport pathways). The fraction of potential growth that can be supported is calculated as the ratio of the carbohydrate available after maintenance respiration to the sum of carbohydrate requirements for potential growth of all the sinks. Since this fraction is the same for all sinks, variations in relative growth rates between organs depend on variations in the daily potential growth of each sink.

Orientation of branching and growth, which determines the geometry of the root system, is not specified in the present model, since such parameters are assumed to be, in a first approximation, unaffected by assimilate availability.

Root growth potential

Determination of the potential elongation rate for each root is a key point in modelling root system growth response to assimilate availability. Models with potential demand functions propose the biomass (or carbon) allocation to be primarily regulated by the potential growth rate of sink organs. However, most of them deal with organs with determinate growth. Therefore, it is possible to establish growth curves under conditions of non-limiting assimilate supply and to assume these growth dynamics to represent potential growth (Marcelis, 1989). In such models, growth potential is thus determined by the ontogeny of the organ or of the whole plant, and often related to temperature. However, such an approach is hardly suitable for root growth, since roots are organs with indeterminate growth, although most of them rapidly cease growing. In rubber, there is extensive variability in both elongation rate and duration within a root type, particularly within acropetal secondary roots and tertiary roots (Le Roux and Pagès, 1994). Therefore, growth curves for faster and longer-term growing roots are not likely to represent the growth potential for a given root type.

Such difficulties led us to seek a morphometrical parameter which could indicate the potential elongation rate of a root at a given time. Previous works have shown a positive correlation between apex diameter and root growth rate (Cahn et al., 1989; Hackett, 1969; review by Coutts, 1987). Moreover, our data (Thaler and Pagès, 1996b) showed that both parameters varied in the same way as related to assimilate availability. Root elongation and apical diameter decreased during shoot growth or under shading, and increased during shoot rest or when shading was removed. The overall apical diameter-elongation rate relationship, for all measured roots on ten seedlings, at each measurement date (Figure 1) showed that the relation was not very close, but that the maximum elongation rate for a given diameter increased with this diameter, particularly for diameters below 0.7 mm. Our hypothesis is that the upper limit of the scatter plot represents the potential

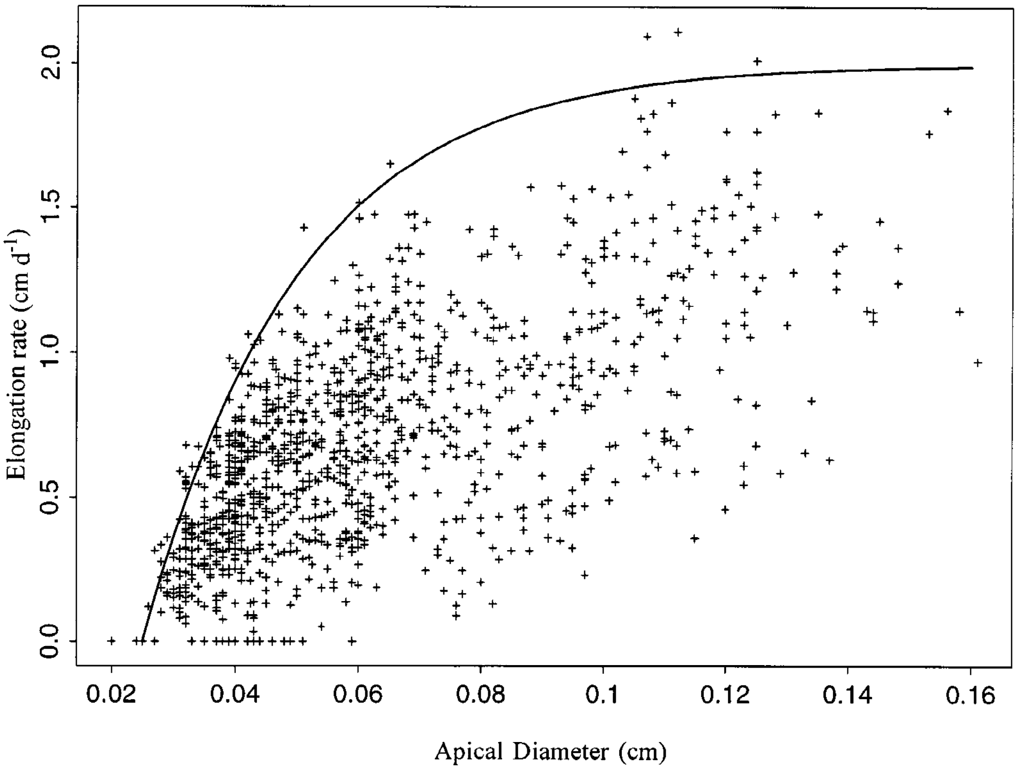

Figure 1. Apical diameter (cm)–Elongation rate (cm d^{-1}) relationship for taproots and secondary roots. Each point (+) represents data for one root at a given date. At each date, 6 roots were measured on eãch plant (10) of the experiment. The envelope curve (–) is a monomolecular function adjusted to 95% quantiles.

elongation rate for a root of a given diameter. Such a hypothesis relies on the observed data, but also on the possible mechanisms which may link root elongation rate to root apical diameter, which were discussed by Thaler and Pagès (1996b). Briefly, we consider the apical diameter to reflect the size of the meristem, and thereby the number of dividing cells (Barlow and Rathfelder, 1984), which represent the demanding units for carbohydrates. Apical width is also related to the development of transport pathways (Feldman and Torrey, 1975), so that carbohydrate demand from roots with a large apex is likely to be higher and to be more easily satisfied than demand from roots with a low diameter.

Since apical diameter varies, the potential elongation rate for each root is not constant, but also depends on assimilate availability. This infers control of sink demand by the supply:demand ratio. Figure 2 shows schematically the model resulting from these concepts.

Model functions

Carbon acquisition

Seed unloading

Seed mass and composition determine the amount of available carbon. This carbon is provided according to a constant rate.

$$C_s = R_s \times M_s \times \Delta t$$

C_s = seed carbon supply (g_{CO_2})
R_s = seed carbon supply rate (d^{-1})
M_s = seed reserves (equivalent CO2, g_{CO_2})
Δt = time step (one day).

Photosynthesis

Daily photosynthesis is proportional to leaf area, between-leaf shading is assumed to be non-signifcant in our conditions. Photosynthesis response to incoming radiation (PAR) could be simulated by a monomolecular function. However, in the present version of the model, photosynthesis is described by a

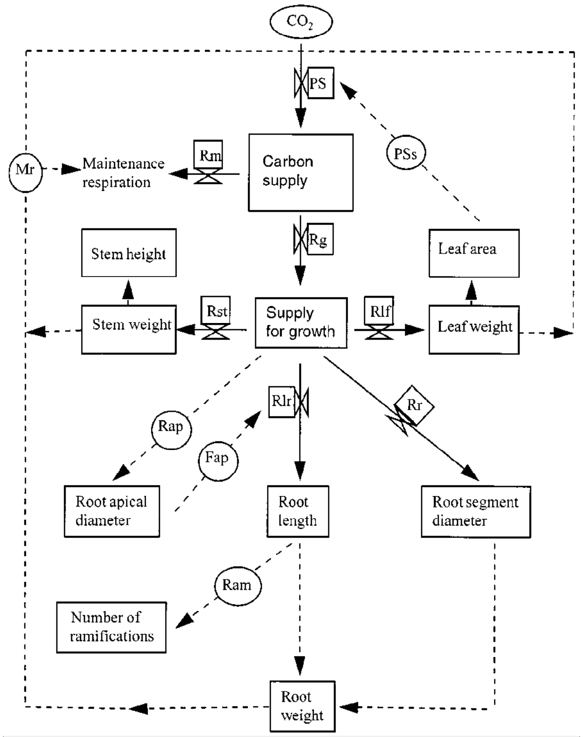

Figure 2. Schematic representation of the model. State variables are represented in rectangles. Solid lines represent carbon fluxes controlled by allocation rates, represented by valves: Rate of carbon allocation to maintenance respiration (R_m), to growth (R_g) to stem growth (R_{st}), to leaf growth (R_{lf}) to root elongation (R_{lr}), to root radial growth (R_r). Dotted lines represent information fluxes. Functions using auxiliary, variables are represented in ellipses: M_r = maintenance respiration; PS$_s$ = specific photosynthetic activity; R_{ap} = diameter evolution rate; F_{ap} = apical diameter-elongation rate function; R_{am} = ramification function.

daily fixed specifc rate whose variations reflect light changes.

$$C_{ps} = LA \times PS \times \Delta t$$

C_{ps} = photosynthesis carbon supply (g_{CO_2})
LA = leaf area (cm^2)
PS = photosynthesis specific rate (g_{CO_2} cm^{-2} d^{-1}).

For each new growth unit, it was assumed that leaves photosynthesize only when they begin to erect (end of stage C, i.e. about 5 days after the date of maximum growth). In fact, their previous drooping habit limits their ability to intercept light radiation.

Reserves

At each time lapse, when the sum of demands is lower than supply, the exceeding carbon is stored. The reserves are released according to a constant rate.

$$C_r = R_r \times M_r \times \Delta t$$

C$_r$ = supply of carbon from reserves (g_{CO_2})
R$_r$ = rate of carbon supply from reserves (d^{-1})
M$_r$ = mass of reserves (g_{CO_2}).

Carbon allocation

Carbon originating from photosynthesis, seed and reserves supplies a common carbon pool. A part of this pool is directed towards maintenance respiration requirements, before supplying carbon for growth. Maintenance respiration is proportional to dry mass.

$$R = R_m \times M \times \Delta t$$

R = maintenance respiration rate (g_{CO_2})
R$_m$ = specific maintenance respiration rate (g_{CO_2} $g_{CO_2}^{-1}$ d^{-1})
M = dry mass (g_{CO_2});

Different R$_m$ are considered for the different parts of the plant: leaf, stem, root. The remaining carbon constitutes the carbon available for growth. Growth rate calculation depends on the chosen allocation rule. With priorities, the complete amount of carbon required for the growth of the successive sinks is subtracted from the carbon pool until the remaining fraction becomes lower than demand of the actual sink. The remaining amount is used to achieve a part of the potential growth of this sink, whereas demands of the following sinks are not satisfied. Without priorities, the current growth rate of each sink is calculated at each time lapse as:

$$G = G_p \times (C_s + C_r + C_{ps} - R)/\Sigma \text{ Demands}$$

G = current growth
G$_p$ = potential growth.

Shoot potential growth

Stem potential elongation and leaf potential extension are described by empirical relations fitted to observed (periodic) growth. For each growth unit (GU), a logistic function is used to model leaf area and another for stem elongation:

$$LA = LA_{max}/(1 + \exp^{(-Bla(T-T_0))})$$

LA = leaf area (cm^2)
LA_{max} = maximum leaf area (cm^2)
B_{la} = initial relative growth increment (d^{-1})
T = time (d)
T_0 = date for maximum growth rate (d).

Leaf area increase is multiplied by current leaf specific mass to determine leaf mass increase, whereas stem elongation is converted into volume increase and then into mass growth, as functions of diameter and volumic mass. An efficiency term is used to convert the demands in dry mass into CO_2. This term also includes growth respiration.

Stem potential radial growth and leaf specifc mass potential growth are assumed to be constant. The period of leaf specific growth is limited.

Root potential growth

According to our hypothesis, the diameter of the apex determines the potential elongation rate of any root. This potential is evaluated by a monomolecular function fitted to the upper limit of the apical diameter-elongation rate scatter plot:

$$E_p = E_{max} \times (1 - \exp^{(-B_r(D-D_0)/E_{\max})})$$

E_p = Potential elongation rate (cm)
E_{max} = maximum elongation rate for all roots (cm)
B_r = initial slope (cm cm^{-1})
D = diameter of the root (cm)
D_0 = threshold diameter below which the root does not elongate (cm).

Evolution of root potential growth (Figure 3)

Variations in apical diameter are simulated by successive functions.

During primordium development. For each root type, a potential initial (at emergence date) diameter is defined. The ratio of this initial diameter to the time lapse between primordium initiation and emergence determines a daily potential diameter increment. When assimilate supply is higher than demand, the primordium grows at its potential rate. When demand is higher than supply, a proportion (determined by allocation rules) of the potential increment is achieved. If the diameter at the emergence date is below a fixed threshold, the root fails to emerge.

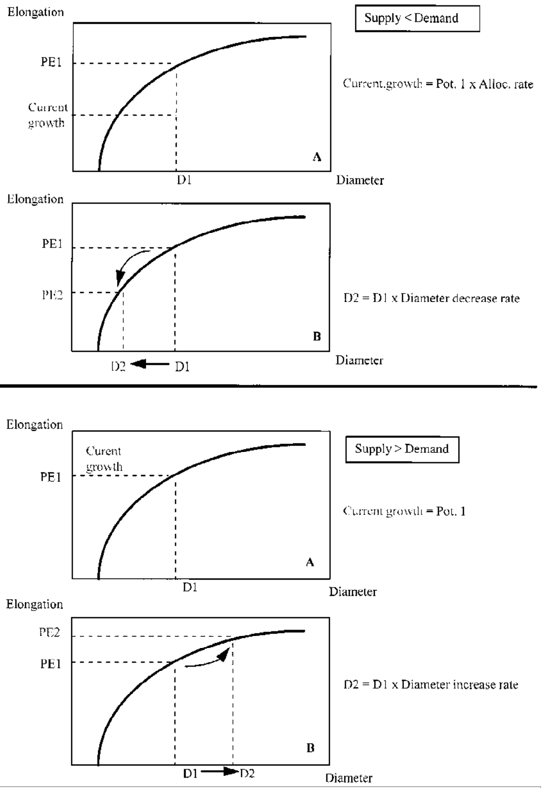

Figure 3. Illustration of the evolution of apical diameter, potential elongation and current elongation. The solid line represents the apical diameter-potential elongation relationship. When supply < demand: A – Current growth achieved by a root with a diameter D1 corresponding to an elongation potential PE1. B – Decrease of the diameter from D1 to D2, conferring an elongation potential PE2 (<PE1) for the next time step. When supply > demand: A – Current growth equal to the potential elongation (PE1) allowed by the diameter D1. B – Increase of the diameter from D1 to D2, conferring an elongation potential PE2 (>PE1) for the next time step.

After emergence. From its value at emergence, the diameter for each root will increase when the supply:demand ratio is above a given threshold, or decrease when this ratio is below another threshold. These thresholds and the (constant) increasing and decreasing rates are input parameters of the model. Thereby, starting from an initial value depending on root type, the potential elongation rate for all roots within the system will vary following a single rule. Growth dynamics of any root is so controlled by a two step variation:

- variation in the proportion of potential growth actually achieved
- variation in the potential growth itself.

Radial growth. For each root type, a constant rate of potential radial growth is determined.

Model parametrization

Estimation of the typical parameters of the model was based on different sources: data from our experiments, parameters used in the rubber tree architectural model (Pagès et al., 1995), and bibliographic data. The material and methods used in our experiments were described in Thaler and Pagès (1996a,b, 1997).

Seed mass

Samples of the seeds used in our experiments were weighed (without seedcoat). In order to convert dry mass values into CO_2 equivalent, we used, for all the organs, an estimated concentration of 0.45 g_c g_{DM}^{-1} (Grossman and Dejong, 1994), which corresponds to 1.65 $g_{CO_2} g_{DM}^{-1}$.

Seed supply rate

Maximum growth rates (in mass) were estimated on young seedlings grown in pots, during development of the first growth unit, when all carbohydrates originated from the seed (data not shown). The maximum rate of dry matter inflow was ca. 0.15 g_{DM} d^{-1} which corresponds to ca. 0.25 $g_{CO_2} d^{-1}$. Assuming an initial seed reserve of 2.8 g_{CO_2}, the daily release rate can be estimated as 0.25/2.8 = 0.09. The simplified rate used was 0.1 d^{-1}.

Reserves supply rate

This coefficient was assumed to be the same as the seed release rate (0.1 d^{-1}).

Photosynthesis specific activity

Photosynthesis was measured in a growth chamber (Thaler and Pagès, 1996b) with an open leaf chamber analyser (ADC, LC4 type, Herts, UK). Considering an incoming photosynthetic photon flux of 400 μmol m^{-2} s^{-1}, mean specific daily photosynthesis was estimated at 0.0014 $g_{CO_2} cm^{-2}$ d^{-1}.

Stem specific mass

This parameter was calculated on the basis of weight, diameter and height measurements for the different growth units. Mean specific mass was 0.29±0.04 g cm^{-3} (range: 0.22–0.37). The default value is 0.30 g cm^{-3}.

Initial apical diameter of the stem and potential radial growth

Radial growth of the stem was measured by displacement sensors (LVDTs) (Huguet, 1985), for a sample of six seedlings grown in pots. Growth rate (range; 0.002–0.006 cm d^{-1}) was nearly constant for a given seedling, during this 25-day experiment. We used an initial diameter of 0.28 cm and a potential growth rate of 0.004 cm d^{-1}.

Maintenance respiration rate

Values were obtained from the bibliography (Amthor, 1989). These data indicate large variations in root maintenance respiration rate, especially as a result of the importance of respiration related to active uptake processes, which is not always taken into account. It is worth mentioning that there are no available estimation of root maintenance respiration for trees (Buwalda, 1993). We therefore chose a uniform maintenance respiration rate for the whole plant (0.02 g_{CO_2} g_{DM}^{-1}).

Dry mass-CO_2 conversion

This coefficient integrates the conversion of dry matter into CO_2, with a concentration estimated at 0.45 g_{CO_2} g_{DM}^{-1} for all the compartments, as well as a growth efficiency coefficient that accounts for growth respiration. According to calculations of Kiwi root growth respiration by the elementary analysis method (Walton and Fowke, 1993) and to mean values for this parameter (Amthor, 1989), we chose an efficiency of 0.75, hence a coefficient of conversion of 2.02 g_{CO_2} g_{DM}^{-1}.

Description of GU growth dynamics

Logistic model parameters were chosen in order to achieve target growths in leaf area and in stem height, according to the chosen assimilate allocation rule. Calibration parameters for these functions were obtained, for each GU, from the dynamics measured during our trials (Example in Table 1). For each growth flush, the asymptotic value (height or maximum area), the date of maximum growth and the initial relative growth increment are defined as input parameters.

Leaf specifc mass

Leaf area and mass were measured according to the stage of development of plants in pots and in root observation boxes. At the end of leaf expansion, leaf specific mass was quite constant (0.0030 g cm^{-2}). Thereafter, this parameter showed a greater variability,

Table 1. Parameter values and initial values of state variables used to simulate the development of a typical rubber seedling, with 3 growth units

CARBON INPUT				
M_s	Seed initial reserves g_{CO_2}	2.8		
R_s	Seed supply rate (d^{-1})	0.1		
R_r	Reserves supply rate (d^{-1})	0.1		
PS	Specific photosynthesis ($g_{CO_2}\,cm^{-2}\,d^{-1}$)	0.0014		
SHOOT DEVELOPMENT				
Overall parameters				
TC_s	Transformation coefficient: demand DM–demand$_{CO_2}$	2.2		
R_{ms}	Maintenance respiration rate ($g_{CO_2}\,g_{DM}^{-1}$)	0.02		
D_{ens}	Stem wood density ($g\,cm^{-3}$)	0.004		
D_{is}	Initial stem apical diameter (cm)	0.28		
R_{sd}	Potential diameter growth ($cm\,d^{-1}$)	0.0004		
M_{la}	Leaf specific mass ($g\,cm^{-2}$)	0.0030		
R_{la}	Leaf specific mass potential growth ($g\,cm^{-2}\,d^{-1}$)	0.0002		
Parameters specified per growth unit				
Stem		GU 1	GU 2	GU 3
$L_{\max}$	Maximum length (cm)	35	20	17
B_s	Initial relative growth increment (d^{-1})	0.7	0.6	0.6
T_{0s}	Date for maximal growth rate (d)	5	32	62
T_{0rs}	Date for the start of radial growth (d)	8	35	65
Leaf				
$LA_{\max}$	Maximum leaf area (cm^2)	190	190	200
B_{la}	Initial relative growth increment (d^{-1})	0.51	0.50	0.55
T_{0la}	Date of maximum growth rate (d)	11	36	68
T_{0ps}	Start of photosynthesis (d)	14	39	71
T_{0smg}	Start of specific mass growth (d)	21	46	78
T_{Fsmg}	End of specific mass growth (d)	36	61	93
ROOTS				
Overall parameters				
ESR	Number of early secondary roots	12		
D_{ensr}	Root wood density ($g\,cm^{-3}$)	0.28		
TC_r	Transformation coefficient: demand CO_2/demand$_{DM}$	2.2		
R_{mr}	Maintenance respiration rate ($g_{CO_2}\,g_{DM}$)	0.02		
E_{max}	Maximum potential elongation rate ($cm\,d^{-1}$)	1.70		
B_r	Initial slope of the Elongation rate-diameter relation (d^{-1})	40		
D_0	Threshold diameter below which elongation stops (cm)	0.025		
AA_{up}	Supply/demand ratio above which apical diameter increases	0.999		
AA_{dw}	Supply/demand ratio below which apical diameter decreases	0.95		
R_{rd}	Apical diameter increase rate	1.015		
R_{rdr}	Apical diameter decrease rate	0.98		
L_{mer}	Meristem length (cm)	0.3		

Parameters specified per root type

Root type		(0) Taproot	(1) LSR	(2) ESR	(3) ASR	(4) R3 /LSR	(5) R3 /ESR	(6) R3 /ASR	(7) R4 /LSR	(8) R4 /ESR	(9) R4 /ASR
D_i	Potential initial apical diameter (cm)	0.20	0.15	0.08	0.05	0.05	0.037	0.037	0.04	0.03	0.03
R_{rs}	Segment diam. potential growth ($cm\,d^{-1}$)	0.0025	0.002	0.001	0.0005	0.0005	0.000	0.000	0.000	0.000	0.000
ZL_i	Inter-branch distance (cm)	0.6	0.6	3.0	3.5	3.5	4.0	4.0	1000	1000	1000
T_{pd}	Primordium development duration (d)	0.0	0.0	0.0	6.0	6.0	6.0	6.0	8.0	8.0	8.0

but considering the maximum mass for each age as a potential value, this potential increased at a rate of ca. 0.00014 g cm^{-2} d^{-1} for 10–15 days. This growth seemed to be limited under shade.

Root volumic mass

We weighed and measured the roots of plants grown in root observation boxes and in pots. The taproot volume was estimated by measuring the diameter every 10 cm, the volume of the secondary roots was estimated assuming a mean diameter of 0.5 mm. According to these measurements root density was quite homogeneous. Although the taproot and some ESR measured were lignifed, unlike most of the ASR, estimated volumic masses were sufficiently similar (0.0026±0.0009 g cm^{-3} for ASR, 0.0030±0.0007 g cm^{-3} for taproot) to choose a single volumic mass (0.0028 g cm^{-3}).

Parameters describing the apical diameter–potential elongation rate relation

The upper limit (95% quantile) of the elongation rate versus apical diameter scatter plot, for all measured roots at each date (Figure 1), was fitted by a monomolecular model. The following three parameters describe this model:

- potential maximum rate ($E_{\max}$): 1.70 cm d^{-1}
- threshold diameter below which elongation stops (D_0): 0.025 cm
- Initial slope (B_r): 40 d^{-1}.

Parameters describing the evolution of apical diameter

The threshold of the supply:demand ratio determining diameter variations (increase or decrease) cannot be measured. The value we used as the increase threshold (0.999) indicated that we considered the diameter to increase when the supply was non-limiting. The decrease threshold (0.95) was a steadying parameter. The variation coefficients (increase: 1.015, decrease: 0.98) were estimated from the diameter variation rate, measured on individual roots (Thaler and Pagès, 1996b). But these parameters showed substantial variability between roots.

Meristem length: 0.3 cm (estimated)

Parameters defined per root type

The initial potential apical diameters were obtained from our measurements, whereas the inter-branch distances and the duration of primordium development were taken from Pagès et al. (1995). The potential growth rate of segment diameter was estimated from diameter measurements on roots of different ages, the potential rate being considered as constant.

Model behaviour

The purpose of this paper was not to present predictive simulations of rubber tree root systems which could be statistically compared to independent data, but to evaluate qualitatively the validity and the limits of the considered hypotheses:

- Competition for assimilates determines root architecture as related to the strength of the different sinks.
- Apical diameter is an efficient indicator of each root's sink strength and its variations can account for the behaviour of the different roots.

We focused on the ability of the model to reproduce the periodicity of root development as related to shoot development and to simulate the differences in sensitivity to assimilate availability depending on root type (Thaler and Pagès, 1996a). We therefore simulated a typical rubber seedling developing three growth units in 77 days, from a mean-sized seed. The parameters we used (table 1) are typical of the seedlings we observed in our growth conditions (Thaler and Pagès, 1996a,b, 1997).

The results shown were produced by the model without priorities, but the hypothesis of the allocation rule does not qualitatively change the behaviour of the model for the considered variables. Slight changes in such parameters as the thresholds and rates of apical diameter variations, the initial slope of the apical diameter-elongation rate relationship, the radial growth rates for the different root types or the seed supply rate were tested to adjust model outputs more closely to the observed data. Nevertheless, whatever the chosen combination of these parameters, it is important to note some permanent trends and limits of the model.

Cumulated elongation per root type

Figure 4a shows the evolution of the cumulated length of the secondary roots. Compared to observed data (which were used to obtain the input parameters), simulated final length tends to be slightly too high. Evolution of the cumulated elongation rates for secondary and tertiary roots (Figure 4b) showed that the simulation of competition for assimilates could reproduce the

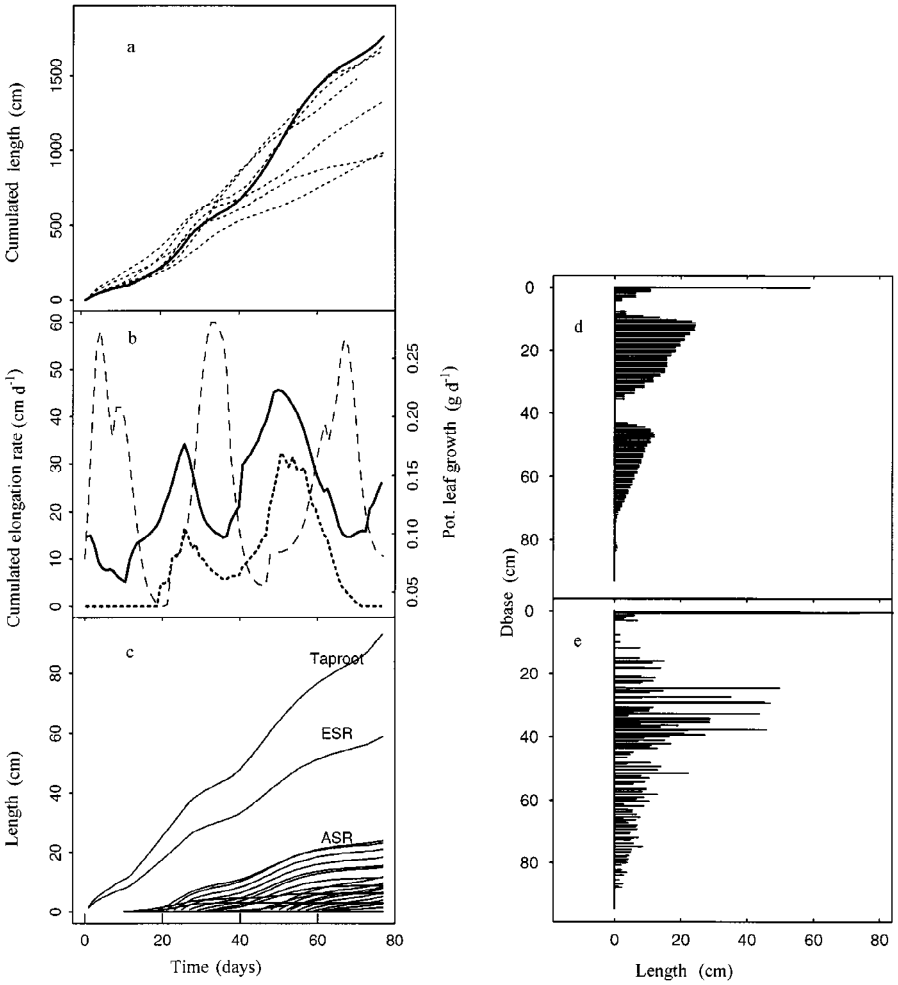

Figure 4. Simulation of a typical seedling (duration 77 days, parameters in Table 1). a – Evolution of cumulated length (cm) for simulated (—) and observed (- - -) secondary roots for 10 plants used to parametrize the model. b – Cumulated elongation rate (cm d^{-1}) for simulated secondary (—) and tertiary (- - -) roots. Leaf potential growth (g d^{-1}) (– – –). c – Evolution of the length (cm) for simulated taproot and secondary roots (one ASR in five is shown). Structure of 77-day old root systems. Horizontal lines represent the final length (cm) of each secondary root as a function of its insertion position (Dbase) on the taproot, shown by the vertical line. d – Simulated. e – Observed.

substantial variations we observed as related to shoot periodic development (Thaler and Pagès, 1996a). The periodicity tallied with observations, with a decrease in elongation rate during shoot growth periods and an increase during shoot rest periods; however, the amplitude of simulated variations tends to be slightly excessive. The lack of inertia of the system partially resulted from the over-straight variations in assimilate input following the development of each new growth unit, when new leaves start to photosynthesize. A progressive increase in photosynthesis with leaf age (Pita et al., 1988) should be introduced to smooth supply variations. Moreover, the demand from each root is fully satisfied until supply becomes lower than overall demand and this prevents simulation of more progressive regulations which could occur when the supply:demand ratio becomes close to 1.

The differences in elongation potential between root types originated in differences in the initial apical diameter. It is worth mentioning that this initial difference was sufficient to simulate the greater sensitivity to assimilate availability shown by tertiary roots. During shoot growth periods, elongation virtually stopped for tertiary roots whereas it was merely depressed for secondary roots (Figure 4b).

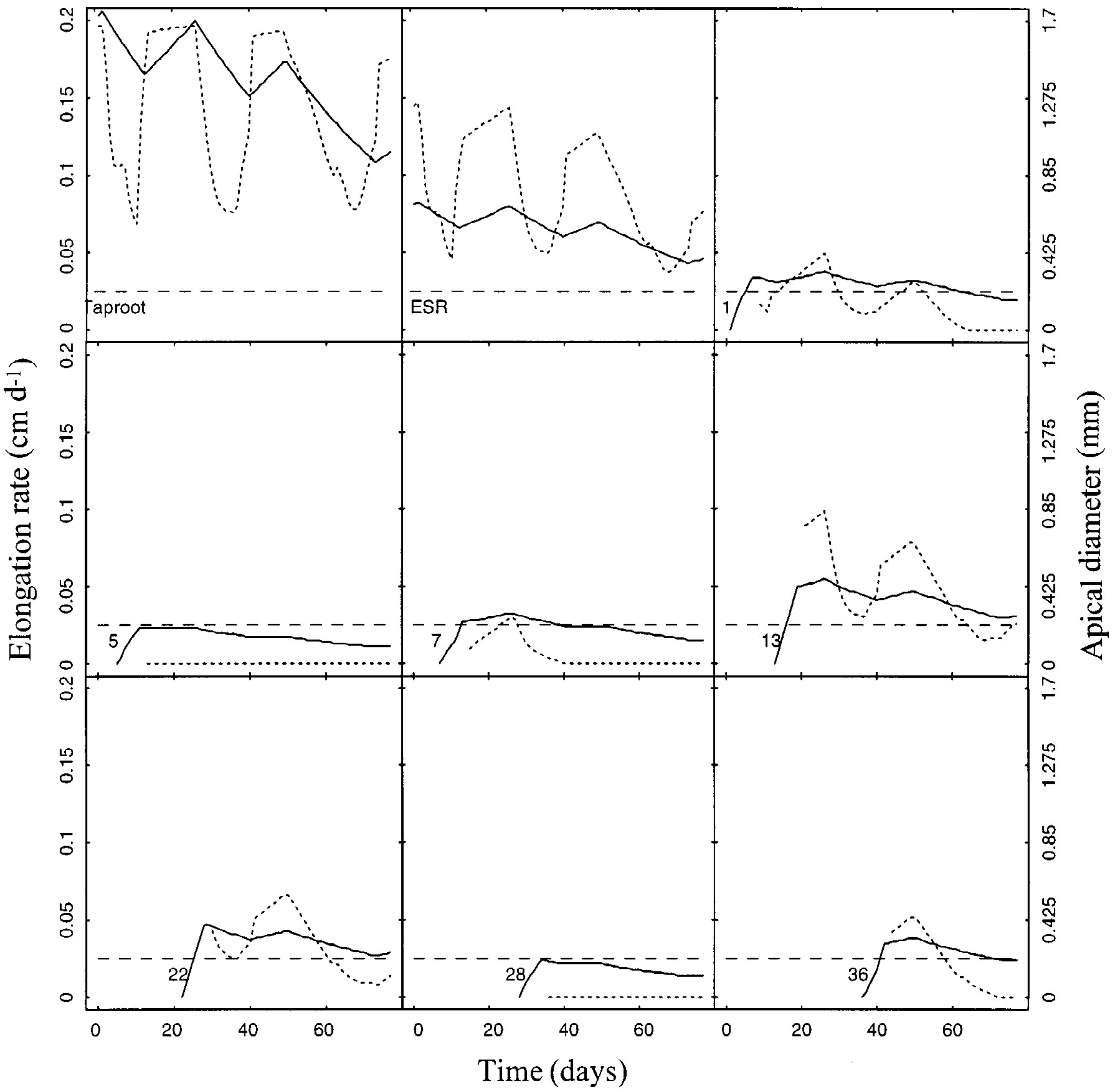

Figure 5. Simulation of the evolution of apical diameter (mm, –) and elongation rate (cm d^{-1}, –) for the taproot, the ESR and a sample of ASR initiated at different dates. The number indicates the initiation date of the root. Primordium development takes 6 days for the ASR. The dashed horizontal line shows the threshold diameter, below which elongation and diameter growth stop.

Invidual root growth curves

Figure 4c shows the evolution of the length of the taproot and individual secondary roots. Differences in potential initial diameter and in primordium development duration resulted in clearly different growth according to root type. Namely, taproot growth was indeterminate and fast, growth of the ESR progressively slowed down, and most of the ASR showed determinate growth. Within a given root type such as the ASR, the temporal variation in assimilate availability related to shoot development resulted in divergent situations (Figure 5). According to their initiation date, simulated ASR aborted when their diameter remained below 0.03 cm at emergence (dates 5 and 28), rapidly showed determinate growth when their diameter fell below this value (dates 7 and 36) or showed longer growth, with a variable rate, until the diameter remained above the threshold (dates 1, 13 and 22). Such temporal variations in the development of ASR enabled simulation of a root system whose structure was similar to observations, the taproot being divided into areas with numerous and often vigorous branches and areas with few and poorly growing branches (Figure 4d, e).

However, the variations in taproot and ESR elongation rate were slightly too great (Figure 5). It was not possible to obtain simultaneously a correct elongation pattern for the taproot and secondary roots. If we changed parameters in order to obtain the greater and more regular taproot growth (by increasing the potential elongation rate or slowing diameter decrease), growth of secondary roots became too great. This phenomenon clearly reveals a limitation of the model resulting from the choice of a single diameter variation rule and a single diameter-elongation rate relationship regardless of root type.

Moreover, since we chose not to introduce stochastic differences between roots, all the roots initiated in the same context (neighbouring roots created during a short period, particularly the ESR) showed exactly the same reactions (Figure 4c, d). In the observed systems, this was not the case: some ESR ceased growing and there were also variations between ASR initiated on the same date (Figure 4e). A larger proportion of roots were in extreme classes (long or short). The structure of our model prevents simulation of such variations. As a consequence, simulated roots must be considered as representations of the mean development achieved by a type of root in a given context.

Discussion

The purpose of our work was to design a model which merged architecture and allocation models. Therefore, this model includes specific features. Compared to allocation models dealing with root development, this one considers each root as an individual sink whose structural properties (branching order, age, connections, diameter) are specified. This specificity confers upon our model the ability to simulate development of the root system not only as a shapeless compartment (Buwalda, 1991; Dick and Dewar, 1992) or as a density profle (Brugge, 1985), but as a structured system of axes. Hence, it provides information on the network properties (extension, topology) of the root system. Compared to architectural models, the description of root growth is completely different, since it is not a predefined time function, but a function of assimilate availability and of each root's sink strength. This provides a link between root architecture and shoot functions. Moreover, this model can restrict the importance of a predefined root typology (whose classes have often artificial limits) since there is a single definition of the growth potential for all root types, the potential initial diameter being the only type-specified parameter. The definition and evaluation of the sink strength is also original since it does not refer to a potential growth fxed a priori (generally estimated by growth curves in non-limiting conditions) but directly depends on the state of the meristem, where growth actually occurs, evaluated by the apical diameter. This notion may be used in the definition of sink strength (which is not always a very precise concept) for many other organs. This model correctly simulates the variations in root development as related to shoot development. It validates thereby the hypothesis that these variations can be explained by competition between roots and shoots for assimilates. Within the root system, simulation of competition can reproduce diversified growth dynamics between axes, using a single rule to define the sink strength of the different roots. Hence it avoids introducing additional, and somehow artificial, rules to distinguish between long-term and short-term growing roots (Aguirrezabal et al., 1994; Jourdan et al., 1995). The gradient of sensitivity to assimilate availability according to root order tallies with observations. The model also simulates the spatial consequences of this competition, namely the heterogeneous distribution of long and short secondary roots along the taproot.

However, some permanent differences between simulations and observations indicate that the hypotheses included in the model are not sufficient and that additional rules have to be introduced. Firstly, we have seen that taproot and secondary root behaviour was too similar in simulations. Some data indicated that the apical diameter-elongation rate relationship was not exactly the same for taproots and secondary roots (Thaler and Pagès, 1996b, 1997). Such differences may originate in the properties of transport pathways. This model does not take into account the pathways between sources and sinks, whereas the number of vascular elements (Le Roux and Pagès, 1994) and sink-source distance are different for the main axis and its branches. The introduction of pathway properties (resistances, storage capacities) into such models seems to be a promising way of obtaining a better understanding of the differences between root types, but also of accounting for local competition between neighbouring axes. In this model, such roots, initiated in the same context, have exactly the same behaviour. By contrast, the occurrence of some ramifications which grow significantly longer than the mean is considered to be of primary importance since they determine the extension of the root system. We have seen that in our model, a slight difference in the initial apical diameter results in large differences in the subsequent growth. There is a high probability that minor variations in assimilate partition could occur between neighbouring primordia at the very first stage of their development (Ganeshaiah and Uma Shaanker, 1994). The introduction of such initial variability is likely to produce the susbtantial differences observed in the growth of neighbouring ramifications. It also seems worth linking the initial diameter of a given axis to the diameter of its mother root, since previous work pointed out that vigorous roots tend to have numerous and also vigorous ramifications (Le Roux and Pagès, 1994).

A more fundamental question concerns the definition of sink strength as related to meristem characteristics. In order to progress in this direction additional research will have to determine cell growth and proliferation pattern (particularly the occurrence and position of cell division which result in new cell files) as related to assimilate availability (Barlow and Adam, 1989). Such work could provide information for overall research on assimilate partition.

To conclude, this approach suggests a new way by which the root system architectural development can be modelled as related to assimilate availability. The model is therefore a useful tool for investigating shoot-root functional relationship. The effects on root architecture of numerous factors such as shading, competition, root pruning or blockage but also growth compensation under soil constraints may be simulated in this way, hence providing information on their overall influence on root system exploitation ability.

Acknowledgements

We would like to thank Valérie Serra for his expert technical assistance, and Helen Burford for correction of the English manuscript.

References

Aguirrezabal L A N, Deléens E and Tardieu F 1994 Root elongation rate is accounted for by intercepted PPFD and source-sink relations in field and laboratory-grown sunflower. Plant Cell Environ. 17, 443–450.

Aguirrezabal L A N and Tardieu F 1996 An architectural analysis of the elongation of field-grown sunflower root systems. Elements for modelling the effects of temperature and intercepted radiation. J. Exp. Bot. 47, 411–420.

Amthor J S 1989 Respiration and Crop Productivity. Springer Verlag, New York. 215 p.

Barlow P W and Adam J S 1989 Experimental control of cellular patterns in the cortex of tomato roots. *In* Structural and Functional Aspects of Transports in Roots. Eds. B Loughman, O Gasparikova and J Kolek. pp 21–24. Kluwer Academic Publishers, Dordrecht.

Barlow P W and Rathfelder E L 1984 Correlations between the dimensions of different zones of grass root apices, and their implication for morphogenesis and differentiation in roots. Ann. Bot. 53, 249–260.

Berntson G M 1994 Modelling root architecture: are they tradeoffs between efficiency and potential of resource acquisition? New Phytol. 127, 483–493.

Brouwer R 1962 Distribution of dry matter in the plant. Neth. J. Agric. Sci. 10, 361–376.

Brugge R 1985 A mechanistic model of grass root growth and development dependent upon photosynthesis and nitrogen uptake. J. Theor. Biol. 116, 443–467.

Buwalda J G 1991 A mathematical model for carbon acquisition and utilisation by kiwifruit vines. Ecol. Model. 57, 43–64.

Buwalda J G 1993 The carbon cost of root systems of perennial fruit crops. Environ. exp. Bot. 33, 131–140.

Cahn M D, Zobel R W and Bouldin D R 1989 Relationship between root elongation rate and diameter and duration of growth of lateral roots of maize. Plant Soil 119, 271–279.

Caldwell M M 1987 Plant architecture and resource competition. Ecol. Stud. 61, 164–179.

Clausnitzer V and Hopmans J W 1994 Simultaneous modeling of transient three-dimensional root growth and soil water flow. Plant Soil 164, 299–314.

Coutts M P 1987 Developmental processes in tree root systems. Can. J. For. Res. 17, 761–767

Dick J M P and Dewar R C 1992 A mechanistic model of carbohydrate dynamics during adventitious root development in leafy cuttings. Ann. Bot. 70, 371–377.

Diggle A J 1988 ROOTMAP – a model in three-dimensional coordinates of the growth and structure of fibrous root systems. Plant Soil 105, 169–178.

Feldman L J and Torrey J G 1975 The quiescent center and primary vascular tissue pattern formation in cultured roots of *Zea*. Can. J. Bot. 53, 2796–2803.

Fitter A H, Sitckland T I, Harvey M L and Wilson G W 1991 Architectural analysis of plant root systems. I. Architectural correlates of exploitation efficiency. New Phytol. 118, 375–382.

Ganeshaiah K N and Uma Shaanker R 1994 Seed and fruit abortion as a process of self organization among developing sinks. Physiol. Plant. 91, 81–89.

Gary C, Jones J W and Longuenesse J J 1993 Modelling daily changes in specific leaf area of tomato: the contribution of the leaf assimilate pool. Acta Hort. 328, 205–210.

Grossman Y F and Dejong T M 1994 PEACH: a simulation model of reproductive and vegetative growth in peach trees. Tree Physiol. 14, 329–345.

Hackett C 1969 Quantitative aspects of the growth of cereal root systems. *In* Root Growth. Ed. W J Whittington. pp 134–147. Butterworth, London.

Huguet J G 1985 Appréciation de l’état hydrique d’une plante à partir des variations micrométriques de la dimension des fruits ou des tiges au cours de la journée. Agronomie 5, 733–741.

Jourdan C, Rey H and Guédon Y 1995 Architectural analysis and modelling of the branching process of the young oil-palm root system. Plant Soil 177, 63–72.

Le Roux Y and Pagès L 1994 Développement et polymorphisme racinaires chez de jeunes semis d'hévéa (*Hevea brasiliensis*). Can. J. Bot. 72, 924–932.

Logendra S, Putman J D and Janes H W 1990 The influence of light period on carbon partitioning, translocation and growth in tomato. Sci. Hort. 42, 75–83.

Marcelis L F M 1993 Simulation of biomass allocation in greenhouse crops – a review. Acta Hort. 328, 49–67.

Nielsen K L, Lynch J P, Jablokow A G and Curtis P S 1994 Carbon cost of root systems: an architectural approach. Plant Soil 165, 161–169.

Pagès L 1995 Growth patterns of the lateral roots in young oak (*Quercus robur* L.) trees. Relationship with apical diameter. New Phytol. 130, 503–509.

Pagès L and Aries F 1988 SARAH: modèle de simulation de la croissance, du développement, et de l'architecture des systémes racinaires. Agronomie 8, 62–68.

Pagès L, Chadoeuf J and Kervella J 1992 Modélisation stochastique de la croissance et du développement racinaire de jeunes pêchers (*Prunus persica* Batsch). I. Estimation et validation du modèle. Agronomie 12, 447–458.

Pagès L, Jordan M O and Picard D 1989 A simulation model of the three-dimensional architecture of the maize root system. Plant Soil 119, 147–154.

Pagès L, Le Roux Y and Thaler P 1995 Modélisation de l'architecture racinaire. Plant. Rech. Dév. 2, 19–34.

Pita F A O, Cano M A O and Fernandes Lopes N 1988 Regulaçao da fotossintese durante a ontogenia foliar de progenies de *Hevea brasiliensis* e *Hevea pauciflora* submetidas a dois regimes hidricos. Pesq. agr. bras. 23, 1209–1219.

Thaler P and Pagès L 1996a Periodicity in the development of the root system of young rubber trees (*Hevea brasiliensis* Müll.-Arg.): relationship with shoot development. Plant Cell Environ. 19, 56–64.

Thaler P and Pagès L 1996b Root apical diameter an root elongation rate of rubber seedlings (*Hevea brasiliensis*) show parallel responses to photoassimilate availability. Physiol. Plant. 97, 365–371.

Thaler P and Pagès L 1997 Competition within the root system of rubber seedlings (*Hevea brasiliensis*) studied by root pruning and blockage. J. Exp. Bot. 48, 1451–1459.

Walton E F and Fowke P J 1993 Estimating the cost of kiwifruit vine growth. Acta Hort. 328, 121–128

Wardlaw I F 1990 Transley review No 27. The control of carbon partitioning in plants. New Phytol. 116, 341–381.

Wightman F and Thimann K V 1980 Hormonal factors controlling the initiation and development of lateral roots. I. Sources of primordia-inducing substances in the primary root of pea seedlings. Physiol. Plant. 49, 13–20.

Yorke J S and Sagar G R 1970 Distribution of secondary root growth potential in the root system of *Pisum sativum*. Can. J. Bot. 48, 699–704.

Section editor: H Lambers